

Third Sound on Substrates Patterned with Periodic and Random Disorder: Evidence for Classical Wave Localization

D. T. Smith, C. P. Lorenson, R. B. Hallock, K. R. McCall, and R. A. Guyer

Laboratory for Low Temperature Physics, Department of Physics and Astronomy,
University of Massachusetts, Amherst, Massachusetts 01003

(Received 20 November 1987)

We report the results of measurements of the propagation of classical waves in thin helium films adsorbed on silicon substrates with two different scattering patterns. Periodic scattering patterns show band structure; random scattering patterns show classical wave localization in one dimension consistent with theoretical predictions.

PACS numbers: 71.55.Jv, 43.20.+g, 67.40.Yv, 67.70.+n

The localization of Schrödinger waves (e.g., electrons) due to scattering from random static disorder has been studied extensively.¹ The analogous classical wave phenomena (localization of electromagnetic waves, elastic waves, etc.) has only recently commanded attention.²⁻⁶ In this paper, we report the results of experiments⁷ which study the propagation of elastic waves in a one-dimensional system. Our experiments involve the third-sound^{8,9} modes of a thin superfluid ⁴He film adsorbed on a silicon substrate; they permit us to verify quantitative features of the theory of classical wave localization.

Third sound on a thin superfluid ⁴He film is the analog of a shallow water wave or a tidal wave. It is driven not by gravity, but by the van der Waals force between the ⁴He fluid and the substrate on which the fluid resides. For a film of thickness d_4 on a smooth substrate, this mode travels with a velocity C_3 that depends both on the strength of the van der Waals force per unit mass at the surface of the film, $f(d_4)$, and on the film thickness as $C_3^2 = (\langle \rho_s \rangle / \rho) d_4 f(d_4)$. Here $\langle \rho_s \rangle / \rho$ is the effective superfluid density in the helium film.¹⁰ Experimental studies¹¹ of third sound on smooth silicon substrates have verified this expression with $f(d_4) \approx 3a/d_4^4$, where $a = 37$ (layers)³ K is the van der Waals constant for the helium-silicon interaction and d_4 is the distance measured in atomic layers (1 layer = 0.36 nm) between the free surface of the helium film and the substrate. On a roughened silicon substrate,¹¹ third sound travels at $C \leq C_3$ because of the change in the film distribution brought about by surface irregularity. The surface roughness is characterized by the index of refraction $n \equiv C_3/C$, which depends on d_4 .

In the experiments we describe here, patterns of one-dimensional disorder are created by abrading a sequence of strips of width w on an otherwise smooth silicon substrate. N abraded strips constitute a sequence of N scattering units. Each unit of length l_j [Fig. 1(a)] consists of an abraded strip of width w , on which the third sound velocity is C_2 , and a segment of smooth surface, on which the third sound velocity is C_1 , giving $n = C_1/C_2$. The propagation of third sound across the j th unit in

such a system is described by a 2×2 frequency-dependent matrix $T_j(\omega)$, where $T_{11} = T_{22}^* = (\cos\phi + ia \sin\phi)e^{i\theta_j}$, $T_{12} = T_{21}^* = ib \sin(\phi)e^{i\theta_j}$, $\phi = \omega w/C_2$, $\theta_j = \omega \times (l_j - w)/C_1$, and a and b are amplitudes that depend on the index of refraction as $a = (n^2 + 1)/2n$ and $b = (n^2 - 1)/2n$.

Condat and Kirkpatrick³ have studied classical wave localization on systems of this type. For the case of position disorder, i.e., random variation in l_j , they find a localization length $\xi(\omega)$ for modes of frequency ω that is a complicated function of ω , n , w , and the density of scatterers, \bar{l}^{-1} . At low frequency ($\omega w/C_2 \leq 1$, i.e., $\omega/2\pi \leq 50$ kHz), their result¹² reduces to

$$\frac{\xi(\omega)}{\bar{l}} = \left[\frac{C_1}{\omega w} \right]^2 \frac{4}{(n^2 - 1)^2}. \quad (1)$$

Below we report the results of experiments that give qualitative and quantitative support for this prediction.

The experiments are conducted at 1.35 K in a sample chamber cooled by a standard ⁴He refrigerator. The

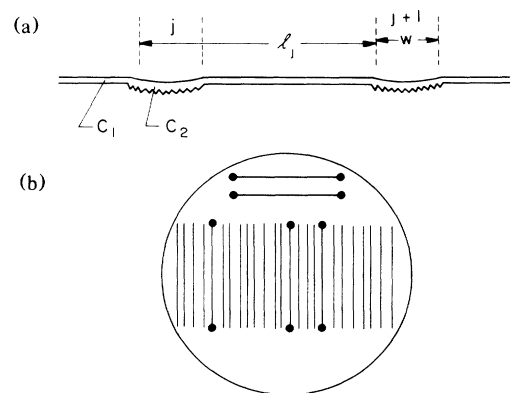


FIG. 1. Schematic representations of abraded substrates. (a) Abraded strips of width w located on a silicon substrate, viewed here in side cross section. (b) Schematic top view of an abraded array located on a Si wafer; visible adjacent to the array is the time-of-flight apparatus used to measure C_1 .

sample chamber contains two Si substrates that are coated with a thin ^4He superfluid film. On one of these, denoted \mathcal{P} , 100 abraded strips are arranged periodically over a length $L=5.0$ cm such that $l_j=500\pm 4.3$ μm . On the other, \mathcal{R} , 100 abraded strips of average separation 500 μm are arranged over the length L with positions chosen from a random number generator. In both cases, the abraded strips have width $w=16\pm 0.6$ μm and are 2.9 cm long.¹³ Third sound is generated and detected with Al transition-edge superconducting bolometers⁸ [2.1 cm \times 150 $\mu\text{m}\times$ (30–40) nm] that are evaporated onto the smooth silicon surface between abraded strips on both \mathcal{P} and \mathcal{R} [Fig. 1(b)]. The generators, located near the middle of the arrays of strips, are driven either by current pulses (~ 1 nJ) or in continuous-wave (cw) mode (~ 20 μW rms). The detectors, at distances of 0.25 and 1.0 cm from the generators, are biased with direct current of nominally 100 μA . Modest changes in these operating parameters do not change the qualitative or quantitative features of the results. It is possible to interchange the role of generator and detector; the important features in the results reported below are invariant to this interchange. In a typical cw experiment, the generator frequency is stepped (~ 3 h) so as to produce third sound in the range $10\text{ Hz} \leq \omega/2\pi \leq 80$ kHz.

During routine operation of an experiment, ^4He could be admitted or removed from the sample chamber so that the film thickness, C_1 , and C_2 could be varied. C_1 , and hence the film thickness, is measured *in situ* with a third-sound time-of-flight apparatus located on a smooth region [Fig. 1(b)] of the silicon substrate.

Measurement of the third-sound amplitude $A(\omega)$ at distances $5\bar{l}=0.25$ cm and $20\bar{l}=1.0$ cm from the generator were made on both the periodic array, reported as $P_5(\omega)$ and $P_{20}(\omega)$, and on the random array, reported as $R_5(\omega)$ and $R_{20}(\omega)$, for films of thickness $3.9 \leq d_4 \leq 11.8$ layers. In Figs. 2(a)–2(c), we show $P_5(\omega)$, $R_5(\omega)$, and $R_{20}(\omega)$, respectively, versus $\omega/2\pi$ for $d_4=5.0$ layers.

Let us begin by looking at the result in Fig. 2(a) for the periodic array. The most apparent feature of $P_5(\omega)$ vs $\omega/2\pi$ is the band structure. We can use the several prominent edges of the band structure and the transmission matrix model described above to estimate the scattering strength of a single abraded strip. For the particular case with $d_4=5.0$ atomic layers shown in Fig. 2(a), we find $n \approx 3.4$.

There is a particularly notable feature in the $P_5(\omega)$ vs $\omega/2\pi$ band structure that suggests that the abraded strips are not all equivalent; the amplitude seen at the high-frequency band edges is suppressed relative to that at the respective low-frequency band edges. Site disorder, i.e., different values of C_2 on different strips, would couple strongly to the modes at the upper band edges (the upper-edge modes have maximum amplitude on the strips), but not at all to the modes at the lower band edges (the lower-edge modes have nodes on the strips).

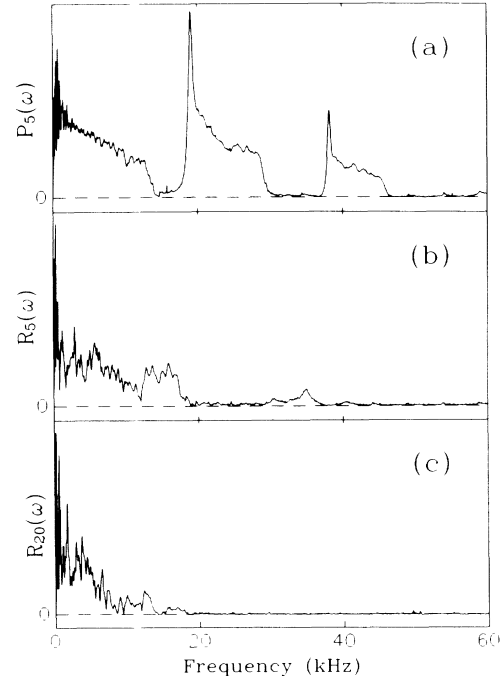


FIG. 2. Amplitude of detected third sound in arbitrary units vs frequency. The amplitudes at distances $5\bar{l}$ and $20\bar{l}$ from the generator are plotted vs $\omega/2\pi$ for a film thickness $d_4=5.0$ layers: (a) \mathcal{P} substrate, $P_5(\omega)$; (b) \mathcal{R} substrate, $R_5(\omega)$; (c) \mathcal{R} substrate, $R_{20}(\omega)$.

We believe the band-edge asymmetry seen in Fig. 2(a) is due to site disorder.¹⁴ Thus, the value of n obtained from the prominent band features is to be regarded as an average value. Because of the presence of site disorder, we might expect to see incipient localization of the third sound on the periodic substrate. Indeed, we believe that the general decay of $P_5(\omega)$ as ω increases within a band is caused in part by this localization. We return to this point later.

Let us now turn to Figs. 2(b) and 2(c), which show the amplitudes $R_5(\omega)$ and $R_{20}(\omega)$ for third-sound propagation on the random array. Examination of $R_5(\omega)$ [$R_{20}(\omega)$] shows that almost no modes at a frequency greater than 20 kHz [15 kHz] are detected 0.25 cm [1.0 cm] away from the generator for the \mathcal{R} array, in strong contrast to what is seen on the \mathcal{P} array. We believe this to be due to localization on length scales less than 0.25 cm [1.0 cm] of most modes at frequencies above 20 kHz [15 kHz] brought about by the position disorder of the abraded strips on the \mathcal{R} array. We are unable to do an experiment on an ensemble of realizations of the system in order to report realization-averaged measurements of this behavior. However, by changing the film thickness, we can change the system, i.e., C_1 and C_2 . While the detailed behavior of $A(\omega)$ vs ω is different for different values of d_4 , we observe the qualitative features seen in Figs. 2(a)–2(c) to be present for every film thickness we have studied.¹⁵

To extract quantitative information from data like that in Figs. 2(b) and 2(c), we carry out an analysis of the data based on the hypothesis that the amplitude measured at distance $m\bar{l}$ away from the generator, $A_m(\omega)$, scales with a single, m -dependent frequency $\bar{\omega}_m(d_4)$, i.e., $A_m(\omega) = g(\omega/\bar{\omega}_m)$. Then, $I_m(\omega) = \int_0^{\omega} A_m(\omega) d\omega = \bar{\omega}_m G(\omega/\bar{\omega}_m)$, where $I_m(\omega)/\bar{\omega}_m$ is a universal function of $\omega/\bar{\omega}_m$. We treat the data for each film thickness as follows: (1) Integrate the $A_m(\omega)$ vs ω data as called for immediately above [see Fig. 3(a)]. (2) Fit $I_m(\omega)$ to a convenient analytic form in order to obtain values for $\bar{\omega}_m$. For convenience, we choose this form to be $I_F(\omega) = B_m[1 - \exp(-\omega/\bar{\omega}_m)]$.

In Table I we tabulate $\bar{\omega}_m$ found from this analysis for $m=5$ and $m=20$ at film thicknesses $3.9 \leq d_4 \leq 11.8$ layers. We note that the values for $\bar{\omega}_m$ are consistent with $1/\sqrt{m}$ scaling as called for by Eq. (1); $\bar{\omega}_5/\bar{\omega}_{20} \approx 2$ for each d_4 . That is, we expect to detect only those modes $\omega \leq \bar{\omega}_m$ that are of a size comparable to or greater than $m\bar{l}$ at a detector located a distance $m\bar{l}$ away from the source; such modes are not localized on a length scale less than $m\bar{l}$. In anticipation of the fact that we are seeing evidence for localization characterized by Eq. (1), we form the quantity $(C_1/w\bar{\omega}_m)^2/m = \gamma$. Measured values for γ are recorded in Table I. To the degree that Eq. (1), an asymptotic relation between the locali-

zation length and ω , correctly describes the dependence of the frequency scaling on m , we expect $\gamma \approx (n^2 - 1)^2/4$, independent of m . From column (d) in Table I, we see that for the four film thicknesses studied, $\gamma_5 \approx \gamma_{20}$ with no systematic deviations. The universal character of $I(\omega)$ is clearly illustrated¹⁶ in Fig. 3(b). We take these results as strong evidence that the third-sound modes on the \mathcal{R} array are localized with a localization length which has the ω dependence of Eq. (1).

Is there an alternative explanation of these results in terms of an ordinary third-sound attenuation mechanism? The qualitative appearance of the \mathcal{R} data, i.e., its "raggedness" as a function of frequency, makes such an explanation implausible. However, in order to make a quantitative assessment of the possible influence of attenuation, we have analyzed the data on the periodic array in two ways. (1) We took the departure of the data on the periodic array from the ideal periodic response to be due entirely to attenuation. We then fit the data with two attenuation coefficients, one describing attenuation on the flat Si surface and the other on the abraded strips. Introduction of these attenuations into a numerical simulation of the behavior of an \mathcal{R} array led to the destruction of all vestiges of localization; the delicate balance of interferences that lead to the "ragged" response characteristic of the data was gone. (2) We took the departure of the data on the periodic array from ideal to be due to a combination of site disorder and attenuation. For example, at $d_4 = 5.0$ layers, a fit to the data leads to an estimate of the strength of the site disorder, $\delta n \approx 1$, and of the attenuation. When this site disorder and attenuation were introduced into a numerical simulation of an \mathcal{R} array, results in qualitative agreement with the data were found. This attenuation *alone*, however, would lead to a decay of the detected signal 1 cm from the source at characteristic frequency $\omega_\beta/2\pi \approx 40$ kHz. This frequency is ~ 8 times larger than the value of $\bar{\omega}_{20}$ reported in

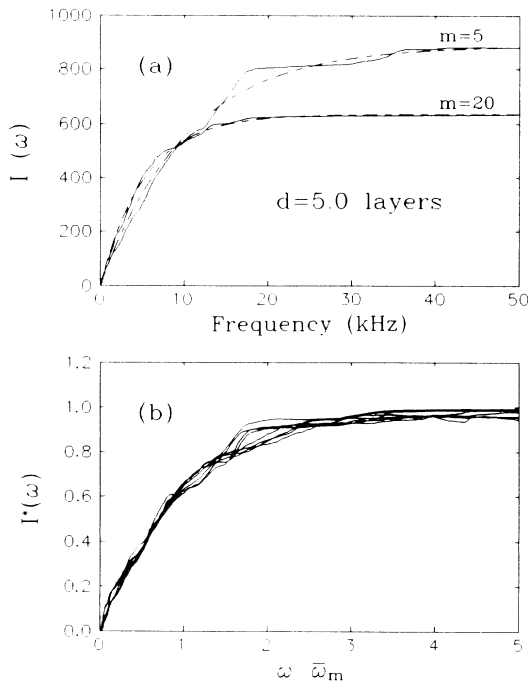


FIG. 3. $I(\omega)$ vs ω . (a) $I(\omega)$ calculated from the data in Figs. 2(b) and 2(c) is plotted vs $\omega/2\pi$. The dashed curves are fits to the form $I_m(\omega) = B_m[1 - \exp(-\omega/\bar{\omega}_m)]$, and yield the values of $\bar{\omega}_m$ in Table I for $d_4 = 5.0$ layers. (b) $I_m^*(\omega) [\equiv I_m(\omega) \text{ normalized (Ref. 16) to 1.0 at large } \omega] \text{ vs } \omega/\bar{\omega}_m$ for $m=5$ and $m=20$ for the four coverages listed in Table I.

TABLE I. Parameters relevant to the analysis of third sound on the \mathcal{R} array; (a) third sound velocity from time-of-flight measurements; (b) distance between generator and detector in units of \bar{l} ; (c) scaling frequency determined from the fit to $I(\omega)$; (d) $\gamma = (C_1/w\bar{\omega}_m)^2/m$, using the data in columns (a) and (c) with $w = 16 \mu\text{m}$.

d_4 (layers)	(a) C_1 (cm/sec)	(b) m	(c) $\bar{\omega}_m/2\pi$ (kHz)	(d) γ
3.9	2529	5	13.9	65
		20	7.4	57
5.0	1945	5	10.3	71
		20	5.3	66
8.5	994	5	5.6	62
		20	2.7	68
11.8	646	5	3.4	72
		20	1.8	63

Table I. Similar ratios of $\omega_p/\bar{\omega}_{20}$ are found for the other thicknesses. Thus, although attenuation is present in this system, we find no evidence that it acts to seriously proscriber our basic conclusion.

As a final point, we note that the magnitude of γ in column (d) of Table I is somewhat larger than we would expect based on Eq. (1). Recall that Eq. (1) is appropriate to the case of position (p) disorder alone. We noted above that there was strong evidence for site (s) disorder on the \mathcal{P} array; an estimate of its magnitude, δn , was found above from analysis of the \mathcal{P} array. Site disorder is also present on the \mathcal{R} array, and will operate as an independent mechanism working to bring about localization. Since site disorder and position disorder are independent, the measured γ reported in column (d) should be the sum of a position contribution and a site contribution. For $d_4=5.0$, we estimate $\gamma_s=24\pm 10$ from analysis of the data on the \mathcal{P} array. Combining this with the value of γ from Table I, we find $\gamma_p\approx 45$. This value of γ_p is consistent with $n\approx 3.8$ in Eq. (1), and compares quite well with the average value we estimate from the band structure, $n\approx 3.4$.

We have shown that third sound on substrates with various scattering patterns can be used to explore qualitative and quantitative features of classical wave localization. Quantitative predictions, $\xi(\omega)\propto 1/\omega^2$ and γ independent of m , are confirmed by the measurements. It appears possible to extend measurements of this type to two-dimensional systems where, in addition to localization, interesting fluctuation and correlation effects have been predicted.¹⁷

This work was motivated by discussions with and calculations¹⁸ by S. Cohen and J. Machta. We have also benefitted from numerous conversations with and unpublished calculations by C. Condat. This work was supported in part by National Science Foundation Grant

No. DMR 85-17939.

¹See, for example, G. Bergmann, Phys. Rep. **107**, 1 (1984); P. A. Lee and T. V. Ramakrishnan, Rev. Mod. Phys. **57**, 287 (1985); D. J. Bishop, D. C. Tsui, and R. C. Dynes, Phys. Rev. Lett. **44**, 1153 (1980).

²Shanjin He and J. D. Maynard, Phys. Rev. Lett. **57**, 3171 (1986).

³C. Condat and T. R. Kirkpatrick, Phys. Rev. B **33**, 3102 (1986).

⁴M. Kohmoto, B. Sutherland, and K. Iguchi, Phys. Rev. Lett. **58**, 2436 (1987).

⁵C. H. Hodges and J. Woodhouse, J. Acoust. Soc. Am. **74**, 894 (1983).

⁶M. Blezons, P. DeVillard, F. Dunlop, E. Guazzelli, O. Parodi, and B. Souillard, to be published.

⁷A preliminary and less quantitative report has appeared: D. T. Smith, C. P. Lorenson, and R. B. Hallock, Jpn. J. Appl. Phys. **26**, Suppl. 26-3, 285 (1987).

⁸I. Rudnick, R. S. Kagiwada, J. C. Fraser, and E. Guyon, Phys. Rev. Lett. **20**, 430 (1968).

⁹K. R. Atkins, Phys. Rev. **113**, 962 (1959).

¹⁰See, for example, S. Putterman, *Superfluid Hydrodynamics* (North-Holland, Amsterdam, 1974), Chap. 5.

¹¹D. T. Smith and R. B. Hallock, Phys. Rev. B **34**, 226 (1986).

¹²Ref. 3 and C. Condat, private communication.

¹³Scanning electron microscopy examination of the abraded strips shows them to be rough concave channels of maximum depth $2\ \mu\text{m}$ and width $16\ \mu\text{m}$ with edge pits of size $\approx 0.5\ \mu\text{m}$.

¹⁴K. R. McCall and R. A. Guyer, to be published.

¹⁵A subsequent experiment with different substrates (and, in particular, a different random pattern) revealed the same qualitative features we report here.

¹⁶To facilitate the required normalization of the data, $I(\omega)$, we have used the multipliers B_m^{-1} generated by the fits $I_F(\omega)$.

¹⁷S. Feng, C. Kane, P. A. Lee, and A. D. Stone, to be published.

¹⁸S. Cohen and J. Machta, Phys. Rev. Lett. **54**, 2242 (1985).